

Brain functional networks extraction based on fMRI artifact removal: single subject and group approaches

Yuhui Du*, Elena A. Allen, Hao He, Jing Sui, *Member IEEE*, and Vince D. Calhoun, *Fellow IEEE*

Abstract—Independent component analysis (ICA) has been widely applied to identify brain functional networks from multiple-subject fMRI. However, the best approach to handle artifacts is not yet clear. In this work, we study and compare two ICA approaches for artifact removal using simulations and real fMRI data. The first approach, recommended by the human connectome project, performs ICA on individual data to remove artifacts, and then applies group ICA on the cleaned data from all subjects. We refer to this approach as Individual ICA artifact Removal Plus Group ICA (IRPG). A second approach, Group Information Guided ICA (GIG-ICA), performs ICA on group data, and then removes the artifact group independent components (ICs), followed by individual subject ICA using the remaining group ICs as spatial references. Experiments demonstrate that GIG-ICA is more accurate in estimation of sources and time courses, more robust to data quality and quantity, and more reliable for identifying networks than IRPG.

I. INTRODUCTION

ICA has an appealing advantage over conventional techniques for studies of functional magnetic resonance imaging (fMRI) data, i.e. no requirement for the hemodynamic response function or regions of interest selection^[1]. Spatial ICA (sICA) is by far the most widely used approach for fMRI, which considers fMRI data as a linear mixture of spatially independent components (ICs) that are mixed by their respective time courses (TCs). The remainder of this paper focuses on sICA denoted by ICA for simplicity.

Although ICA has been successful in the analysis of fMRI data, one of the challenges is in labeling ICs that include not only meaningful functional networks but also various artifacts arising from imaging and physiology activity. Issues like identifying artifacts and selecting the number of sources become more challenging when analyzing multi-subject fMRI.

Two kinds of ICA approaches are usually adopted in fMRI studies with multiple subjects. One kind performs ICA for each subject and then establishes correspondence of ICs across subjects using subjective identification, clustering or cross correlation. However, it is difficult to establish correspondence due to the different ordering of ICs,

especially if the number of components is different. The other kind, referred to as group ICA^[2-4], can establish direct correspondence of ICs across subjects through implementing an ICA on all data and then estimating subject-specific ICs/TCs from group results. Group ICA approaches include spatial concatenation, temporal concatenation^[2,3] and tensor organization methods, though temporal concatenation methods are most widely used. Typical temporal concatenation approaches utilizing either PCA-based^[2] or regression-based^[3,5] back reconstruction capture individual variability well, but may not be optimal for artifacts which can be extremely unique across subjects^[4].

In this paper, we study and compare two approaches for artifact removal based functional networks extraction from multiple-subject ICA of fMRI data. The first approach recommended by the human connectome project^[6], which we call IRPG for Individual ICA artifact Removal Plus Group ICA, implements individual ICA on each subject data, identifies and removes artifact ICs from each ICA result, and then performs group ICA on the reconstructed datasets. The IRPG approach accounts for extreme inter-subject variability in the artifacts, however the difficulties inherent in identifying subject-specific artifact ICs and inaccuracy of the estimated number of ICs may cause problems. This is particularly the case if many subjects are involved, although approaches for training classifiers can help mitigate this to a degree^[6]. The second approach skips the expensive single-subject ICA step and directly applies a variant of group ICA based on a new one-unit ICA with reference algorithm^[7]. This approach, called Group Information Guided ICA (GIG-ICA)^[7], implements ICA on all data, and then uses the non-artifact group ICs as references to compute individual networks. Compared to IRPG, GIG-ICA does not require individual identification of artifact ICs for each subject. Instead, GIG-ICA takes advantage of the fact that components which show similarity among subjects (e.g. the networks of interest) tend to not be corrupted by the unique artifacts^[2] but allows for additional flexibility in individual subjects by re-optimizing the independence using the group maps via a multi-objective function optimization algorithm.

II. METHODS

We first introduce the framework and parameters for IRPG and GIG-ICA, and then describe simulations and real fMRI experiments.

IRPG involves steps: (1) ICA on each individual dataset, (2) identification of subject-specific artifact ICs, (3) individual data reconstruction based on the remaining non-artifact ICs, and (4) group ICA on the reconstructed data from all subjects. Group ICA is implemented by temporal concatenation^[2] with spatio-temporal (dual) regression^[3,5] to be consistent with

* Research supported by NIH.

Yuhui Du is with The Mind Research Network, Albuquerque, NM, 87106, USA and School of Information and Communication Engineering, North University of China, Taiyuan, 030051, China. (corresponding author phone: 505-573-1356, e-mail: ydu@mrn.org and duyuhui@nuc.edu.cn)

Elena A. Allen is with The Mind Research Network, Albuquerque, NM, 87106, USA and K.G. Jebsen Center for Research on Neuropsychiatric Disorders and Department of Biological and Medical Psychology, University of Bergen, Bergen, 5009, Norway. (eallen@mrn.org)

Hao He, Jing Sui, and Vince D. Calhoun are with The Mind Research Network and Dept. of ECE of New Mexico, Albuquerque, NM, 87106, USA. (vcalhoun@unm.edu).

some recent work from the human connectome project^[6]. Some free parameters in IRPG include the number of PCs/ICs in step 1 (I1), the number of PCs in the subject-level PCA of step 4 (I2), and the number of PCs/ICs in the group-level PCA/ICA of step 4 (I3).

GIG-ICA involves steps: (1) application of group level ICA to all subject datasets, (2) identification of artifact group ICs, (3) computation of individual ICs via one-unit ICA with reference algorithm on individual datasets using the non-artifact group ICs as spatial references^[7], and (4) computation of individual TCs using regression. Relevant free parameters in GIG-ICA include the number of PCs in the subject-level PCAs of step 1 (G1), and the number of PCs/ICs in the group-level PCA/ICA of step 1 (G2).

A. Experiments using simulations

Multi-subject fMRI-like data were generated using SimTB toolbox^[8]. For subjects $i = 1 \dots M$ ($M = 10$), simulated datasets were generated under a linear mixture model using C ($C = 8$) source images (148×148 pixels) and associated TCs with certain time points. Rician noise was added to the linear mixture of sources with a specified contrast-to-noise ratio (CNR). Among C sources, some were labeled as non-artifact sources, while others were labeled as artifacts. The j^{th} source of the i^{th} subject is denoted by $S_{i,j}$. When $j = 1, \dots, K$ ($K = 7$), $S_{i,j}$ was non-artifact sources, and when $j = K + 1, \dots, C$, $S_{i,j}$ was artifact sources.

Experiment 1: Effect of data quality and quantity

Simulated ground-truth (GT) sources and their associated TCs of two subjects are shown in Fig. 1. The 8th source with high frequency TC is chosen as the artifact. For different subjects, each of the eight sources was generated through adding subject-specific variability to a common map. In this experiment, datasets with time points of TCs as 150 and different CNRs ranging from 0.5 to 2 were used to evaluate the effect of data quality, and datasets with CNR as 2 and time points of TCs varied from 40 to 120 were used to evaluate the effect of data quantity.

For IRPG, I1 was specified as the true source number C for all subjects, I2 and I3 were set to $C - 1$ reflecting the true number of remaining ICs since a single individual artifact IC was accurately identified and removed by finding the individual IC with the largest absolute value of Pearson correlations to respective artifact template. The artifact template for the i^{th} subject in IRPG was defined as the subject-specific ground-truth (GT) artifact source $S_{i,8}$. For GIG-ICA, both G1 and G2 were set to C . For GIG-ICA, the group level artifact was accurately identified by finding the group IC with the largest absolute value of Pearson correlations to a artifact template T_8 , which was generated by averaging the GT artifact sources across subjects. Here, we define

$$T_j = \frac{1}{M} \sum_{i=1}^M S_{i,j}. \quad (1)$$

To evaluate the accuracy of each estimated individual IC/TC, the absolute value of Pearson correlation coefficient between the IC/TC and its related GT source/TC was computed. The mean of all IC/TC accuracy was calculated to

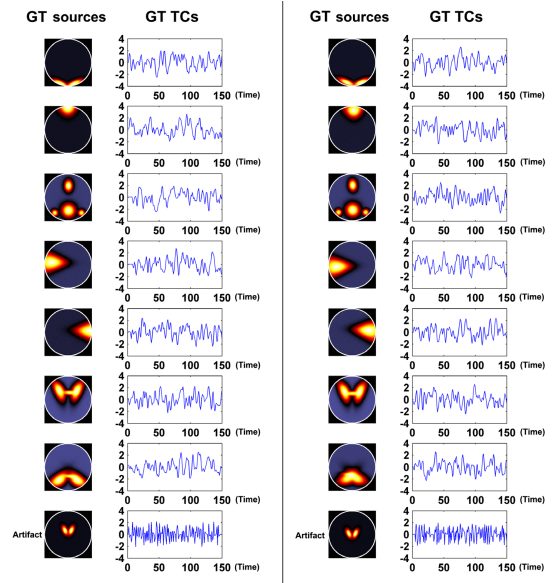


Figure 1. Ground-truth (GT) sources and TCs of two subjects.

reflect overall spatial/temporal accuracy of one subject. The GT source associated with each estimated IC was identified by matching the group ICs and non-artifact templates T_j ($j = 1 \dots 7$). Based on a correlation matrix, each element of which reflects the spatial correlation of one group IC and one T_j , a greedy rule was applied to match group ICs to non-artifact templates one by one, accordingly individual ICs/TCs' corresponding GT sources/TCs were found one by one. In the following experiment, we used a similar approach to evaluate the quality of ICs/TCs estimation.

Experiment 2: Effect of spatially unique artifact

In the experiment 1, corresponding sources of different subjects were simulated by adding subject-specific spatial variation to a common map. However, in real data it is likely that spatially unique sources exist among subjects, particularly for artifacts. Therefore, greatly varied spatial artifacts (the 8th source) with high-frequency TCs were generated for subjects as shown in Fig. 2. In this experiment, CNR was 2 and time points of TCs was 150, and parameters setting of two methods are as same as that in Experiment 1. For IRPG, the artifact IC of each subject was identified correctly by finding the TC with the most high frequency power. For GIG-ICA, the artifact group IC was identified accurately as a group IC that generated high-frequency individual TCs.

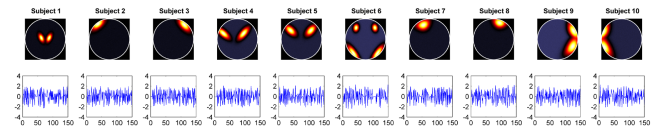


Figure 2. Ground-truth (GT) artifact sources and TCs for ten subjects.

B. Experiment using real fMRI data

Resting fMRI datasets comprising 25 healthy participants with three scans^[9] were preprocessed using SPM8. For each dataset, the first ten images were discarded, and the remaining images were slice-time corrected and realigned to the first volume for head-motion correction. Subsequently, the images

were spatially normalized to the MNI EPI template and spatially smoothed with a 6 mm FWHM Gaussian kernel.

These 75 datasets were then subjected to IRPG and GIG-ICA to extract intrinsic functional networks (INs). Since the estimated maximum and mean number of ICs using Minimum Description Length criteria (MDL), Akaike Information Criterion (AIC), and Kullback–Leibler Information Criterion (KIC) were 45 and 20, respectively, we set I1 to 45, I2 to the minimum number of remaining dimensions after artifact removal, and I3 to 20 with the condition that $I3 < I2$. For GIG-ICA, G1 and G2 were respectively set as same as I1 and I3 for an equivalent comparison. In the group ICA step for both IRPG and GIG-ICA, ICASSO^[10] was used with 20 iterations to find reliable group components.

To automatically identify artifact individual ICs in IRPG, we adopted an approach similar to a method proposed by Bhaganagarapu^[11], and computed seven parameters from each IC and related TC. We define IC_{thr} is the binary 3D map of each z-scored IC after thresholding with $z > 2$. Four parameters include the overlap degree between IC_{thr} and a CSF mask, denoted by O_C , the overlap degree between IC_{thr} and a white matter mask, denoted by O_W , the overlap degree between IC_{thr} and a grey matter mask, denoted by O_G , and IC_{thr} and a brain edge mask, denoted by O_E . Other parameters include smoothness measure of IC_{thr} , denoted as S_A , low frequency to high frequency power ratio of the z-scored TC, denoted as F , and the negative value of derivative sum of power spectrum of the z-scored TC within the low frequency range, denoted as D . We determined separate thresholds for above parameters according to their distributions to identify artifacts, denoted as $Thr\{O_C\}$, $Thr\{O_W\}$, $Thr\{O_G\}$, $Thr\{O_E\}$, $Thr\{S_A\}$, $Thr\{F\}$, and $Thr\{D\}$. ICs were considered as artifacts if $O_C > Thr\{O_C\}$, $O_W > Thr\{O_W\}$, $O_G < Thr\{O_G\}$, $O_E > Thr\{O_E\}$, $S_A < Thr\{S_A\}$, or $F < Thr\{F\}$ and $D < Thr\{D\}$. For GIG-ICA, O_C , O_W , O_G , O_E , and S_A were computed for each group IC. Preliminary individual TCs were calculated using regression, and then the average F and D of corresponding TCs from all datasets, denoted as \bar{F} and \bar{D} , were computed, respectively. Similarly, $Thr\{O_C\}$, $Thr\{O_W\}$, $Thr\{O_G\}$, $Thr\{O_E\}$, $Thr\{S_A\}$, $Thr\{\bar{F}\}$, and $Thr\{\bar{D}\}$ in GIG-ICA were determined to identify and remove artifact group ICs.

To evaluate the reliability of the estimated individual INs, (1), the pair-wise similarity of all individual INs were computed, (2), all individual INs were projected to a plane using t-Distributed Stochastic Neighbor Embedding (t-SNE) method^[12], (3), voxel-wise one-sample t-tests were performed for each IN and the maximum t-value was compared, (4), voxel-wise intra class coefficients (ICCs) between INs from scan 1 and mean INs from scan 2 and 3 were calculated, and the mean ICC of each IN was then computed across voxels within a specific mask including only statistically significant voxels from the one-sample t-tests.

III. RESULTS

A. Experiments using simulations

Experiment 1: Effect of data quality and quantity

As shown in Fig. 3, the accuracy of estimation improves with increasing CNR as well as time points of TCs for both

IRPG and GIG-ICA. However, GIG-ICA showed more reliable and better performance than IRPG, and worked well even in the case of low CNR or few time points of data.

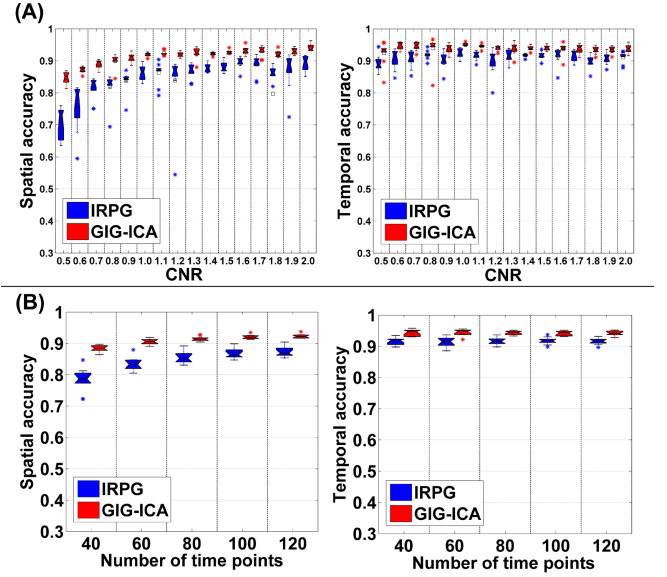


Figure 3. Spatial and temporal accuracy obtained from IRPG and GIG-ICA from (A) datasets with different CNR and (B) datasets with different number of time points of TCs. Each point in a given boxplot corresponds to the mean accuracy of ICs/TCs for one subject.

Experiment 2: Effect of spatially unique artifact

Fig. 4 shows the accuracy results of each individual IC/TC obtained from IRPG and GIG-ICA for all subjects. Even when subjects had spatially unique artifacts, GIG-ICA had a better performance for ICs and a comparable performance for TCs compared to IRPG (mean of temporal accuracy for IRPG and GIG-ICA are 0.905 and 0.902, respectively).

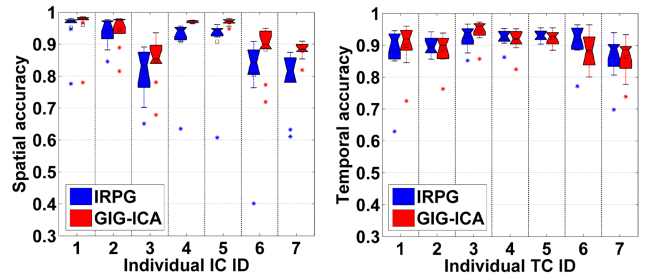


Figure 4. The spatial accuracy of individual ICs and temporal accuracy of individual TCs obtained from IRPG and GIG-ICA. Each point in a given boxplot corresponds to the accuracy of one IC/TC for one subject. The order of ICs in x-axis is as same as that of those non-artifact sources in Fig. 1.

B. Experiment using real fMRI data

In real data, 12 corresponding INs were found and compared between methods. Fig. 5 (A) shows the correlations between all INs of all subjects. Corresponding INs across 75 datasets are relating to a diagonal sub-matrix (size: 75×75), which indicates that INs from GIG-ICA were more spatially consistent. Projection results of all individual ICs are shown in Fig. 5(B), which illustrates that corresponding INs from GIG-ICA presented a more tightly clustered pattern while INs estimated from IRPG presented mixed pattern to some degree. The maximum t-value of each IN was larger (Fig. 5(C)) and mean ICC values were greater (Fig. 5(D)) in GIG-ICA. One-sample t-test results of networks (FDR corrected $p < 0.01$)

are shown in Fig. 6. These results demonstrate that networks obtained from GIG-ICA had higher reliability than those computed by IRPG.

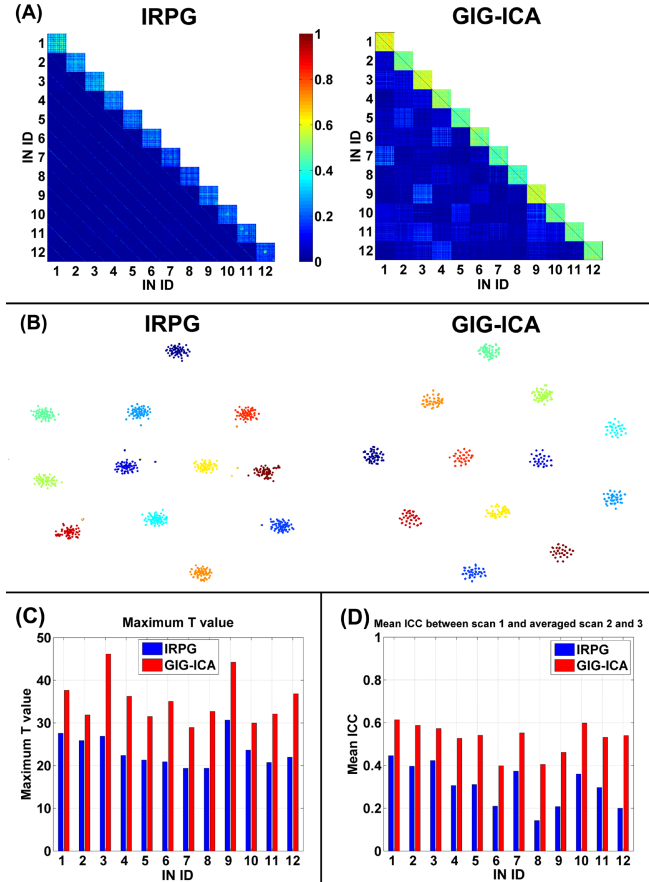


Figure 5. (A) The correlation matrix of individual INs from IRPG and GIG-ICA. (B) Projection of individual INs estimated by IRPG and GIG-ICA. Points with the same color denote corresponding INs from different datasets. Different colors denote different INs. (C) Maximum t value of each IN. (D) Mean ICC between scan 1 and the averaged scan 2 and scan 3 for each IN.



Figure 6. One-sample t-test statistics for the matched 12 networks, thresholded at $p < 0.01$ with FDR correction for IRPG and GIG-ICA. The order of ICs (INs) is as same as that in Fig. 5.

IV. CONCLUSION

In this paper, we address two approaches for functional networks extraction based on artifact removal from

multi-subject ICA of fMRI. IRPG first removes artifact ICs from separate individual ICA results, and then implements a traditional group ICA on cleaned data from all subjects. GIG-ICA removes group level artifacts after an ICA on all subject datasets, and then estimates subject-specific ICs with non-artifact group ICs as references. Simulation based experiments demonstrate that GIG-ICA showed better performance than IRPG, even in the case where single-subject artifact removal was perfect for IPRG and where subjects had spatially unique artifacts. Furthermore, simulation based experiments also reveal that IRPG was more sensitive to data quality and quantity compared to GIG-ICA. Experiment using test-retest fMRI data illustrates that GIG-ICA generated more reliable brain networks with less noise. In summary, GIG-ICA is considerably more accurate in estimation of sources and time courses, more robust to changes in data quality and quantity, and more straightforward to apply to functional networks extraction.

ACKNOWLEDGMENT

This work was partially supported by National Institutes of Health grants R01EB006841, National Sciences Foundation grants 1016619, and the Centers of Biomedical Research Excellence (COBRE) grant 5P20RR021938/P20GM103472 (to Calhoun VD). EAA was supported by the K.G. Jebsen Foundation.

REFERENCES

- [1] Y. H. Du, H. M. Li, H. Wu, and Y. Fan, "Identification of subject specific and functional consistent ROIs using semi-supervised learning," *SPIE medical imaging*, vol. 8314AS, 2012.
- [2] V. D. Calhoun, T. Adali, G. D. Pearlson and J. J. Pekar, "A method for making group inferences from functional MRI data using independent component analysis," *Hum Brain Mapp*, vol. 14(3), pp. 140-151, 2001.
- [3] C. Beckmann, C. Mackay, N. Filippini and S. Smith, "Group comparison of resting-state FMRI data using multi-subject ICA and dual regression," *Neuroimage*, vol. 47 Supplement 1, pp. S148, 2009.
- [4] V. D. Calhoun and T. Adali, "Multisubject independent component analysis of fMRI: a decade of intrinsic networks, default mode, and neurodiagnostic discovery," *IEEE Rev Biomed Eng*, vol. 5, pp. 60-73, 2012.
- [5] V. D. Calhoun, J. J. Pekar and G. D. Pearlson, "Alcohol intoxication effects on simulated driving: Exploring alcohol-dose effects on brain activation using functional MRI," *Neuropsychopharmacology*, vol. 29(11), pp. 2097-2107, 2004.
- [6] S. M. Smith, et al., "Resting-state fMRI in the Human Connectome Project," *Neuroimage*, vol. 80, pp. 144-168, 2013.
- [7] Y. H. Du and Y. Fan, "Group information guided ICA for fMRI data analysis," *Neuroimage*, vol. 69, pp. 157-197, 2013.
- [8] E. A. Allen, E. B. Erhardt, Y. Wei, T. Eichele and V. D. Calhoun, "Capturing inter-subject variability with group independent component analysis of fMRI data: a simulation study," *Neuroimage*, vol. 59(4), pp. 4141-4159, 2012.
- [9] X. N. Zuo, C. Kelly, J. S. Adelstein, D. F. Klein, F. X. Castellanos and M. P. Milham, "Reliable intrinsic connectivity networks: Test-retest evaluation using ICA and dual regression approach," *Neuroimage*, vol. 49(3), pp. 2163-2177, 2010.
- [10] J. Himberg, A. Hyvarinen and F. Esposito, "Validating the independent components of neuroimaging time series via clustering and visualization," *Neuroimage*, vol. 22(3), pp. 1214-1222, 2004.
- [11] K. Bhaganagarapu, G. D. Jackson and D. F. Abbott, "An automated method for identifying artifact in independent component analysis of resting-state FMRI," *Front Hum Neurosci*, vol. 7, 343, 2013.
- [12] L. van der Maaten, and G. Hinton, "Visualizing Data using t-SNE," *Journal of Machine Learning Research*, vol. 9, pp. 2579-2605, 2008.